Journal of Structural Geology 33 (2011) 633–643

Contents lists available at ScienceDirect

Journal of Structural Geology

journal homepage: www.elsevier.com/locate/jsg

The formation and growth of pressure solution seams in clastic rocks: A field and analytical study

Filippo Nenna*, Atilla Aydin

Rock Fracture Project, Department of Geological and Environmental Sciences, Stanford University, CA 94305, USA

ARTICLE INFO

Article history:
Received 1 April 2010
Received in revised form
18 January 2011
Accepted 29 January 2011
Available online 22 February 2011

Keywords:
Pressure solution
Pressure solution seam
Inter-granular pressure solution
Pressure solution growth
Pressure solution zone

ABSTRACT

Pressure solution seams (PSSs) are closing mode structures of localised dissolution resulting in a volume reduction. We present new observations constraining the processes by which PSSs initiate and grow in low porosity clastic rocks from southern Ireland. PSSs initiate as inter-granular PSSs at quartz grain to grain contacts. As quartz dissolves, clay remains as a residue along the contacts as well as filling the adjacent pores to form incipient PSSs involving multiple grain boundaries. Further lengthening and thickening occurs by lateral linkage and transverse coalescence of neighbouring segments of incipient PSSs. Multiple PSS segments are observed to concentrate in thin tabular zones that appear as single macroscopic PSSs visible in hand samples. Published numerical modelling results show the ability of both lateral and transverse growth of PSSs due to the presence of asperities on their flanks, which confirm our interpretations based on our laboratory and field observations.

1. Introduction

Pressure solution seams (PSSs) are closing mode structures of localised grain dissolution that form perpendicular to maximum compressive stress (Weyl, 1959; Fletcher and Pollard, 1981; Koehen et al., 2007). PSSs can form parallel to bedding in response to overburden pressure, and at high angle or perpendicular to bedding due to tectonic compression (Dunnington, 1967; Onasch, 1994; Graham Wall et al., 2006; Baron and Parnell, 2007; Agosta and Aydin, 2006). Early studies reported the presence of PSSs primarily in carbonate rocks where the dissolution of calcite often forms stylolites that have sutured geometries (Stockdale, 1922). However, since the recognition of pressure solution in clastic material, it has become a focus of many studies including sandstone hydrocarbon reservoir compaction (Baron and Parnell, 2007; Yang, 2000), sandstone cementation (Heald, 1959; Bjørlykke and Egeberg, 1995; Oelkers et al., 1996) and strain analysis (Onasch et al., 1998).

A conceptual model of pressure solution consists of three stages (Weyl, 1959; Renard et al., 1997; Groshong, 1988; Koehn et al., 2006): (a) dissolution and grain interpenetration driven primarily by effective stress at grain contacts (Sorby, 1864; Rossi et al., 2007); (b) diffusion/dispersion of dissolved material from areas of high local stress, facilitated by chemical potential and fluid-flux (Sprunt and Nur, 1976; Hickman and Evans, 1995; Lehner, 1995); (c) precipitation of materials in areas of lower local compressive stress (Fig. 1). This process is a time-dependant slow diffusive mass transfer process in which the slowest of the three stages controls the overall deformation rate (Rutter, 1983; Renard and Dsythe, 2003; Gratier et al., 2009).

The dissolution rate of two grains in contact with each other is driven by the local stress conditions at the grain contacts, temperature, the presence of fluid on the surface of the grains and the chemical potential of the dissolving material: i.e. the contrast in concentration of the material between the water film at the grain contact and that of the fluid away from the contact. Presence of a film of water caught between two grains under compressive stresses is required as both a solvent and a transportation agent for the dissolved material (Weyl, 1959; Rutter, 1983; Renard et al., 1997; Rossi et al., 2007). Precipitation occurs away from the contact where local stresses are lower, often adjacent to the free surface closest to the grain contact. Greater amounts of fluid present in the pore spaces allows for material to be transported further from the source, and perhaps even out of the system completely.

The process of grain dissolution and the subsequent precipitation of material in pore space are important diagenetic modifications of sedimentary rocks and act to reduce porosity and permeability locally in the host rock (Bjørlykke and Egeberg, 1995), and especially within the PSSs (Carrio-Schaffhauser et al., 1990). Experimental studies on sandstones have reported bulk porosity

* Corresponding author.
E-mail address: fnenna@stanford.edu (F. Nenna).

0191-8141/$ – see front matter © 2011 Elsevier Ltd. All rights reserved.
doi:10.1016/j.jsg.2011.01.014

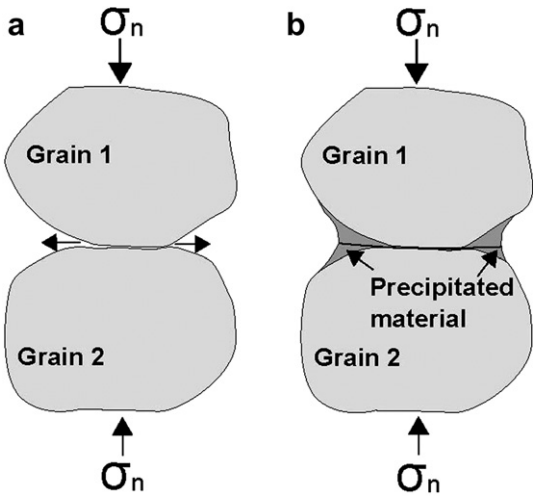

Fig. 1. A conceptual model of pressure solution formation consists of (a) dissolution and grain interpenetration driven by effective stress at grain contacts and diffusion/dispersion of dissolved material from areas of high local stress and (b) precipitation of material in areas of lower local compressive stress (Renard et al., 1997).

reduction by pressure solution alone of over 50% (Sprunt and Nur, 1976). Therefore the timing, nature and distributions of PSSs, and the related veins within reservoir rocks will have significant implications for fluid flow. Furthermore, Dunnington (1967) suggested that the presence of oil in pore spaces could hinder the formation of PSSs, as mineral grains are much less soluble in oil than water.

Though PSSs have been observed by many previous workers (Stockdale, 1922; Railsback, 1993; Bathurst, 1995; Baron and Parnell, 2007), little has been done to explain the growth of, and interaction between, these structures. In this contribution, we characterise the geometry, roughness and elemental composition of PSSs in increasing detail in clastic material using outcrop, hand sample and thin section scale observations. We then delineate the mechanisms for growth and coalescence of PSSs and evaluate them to numerical models of localised volume reduction structures (LVRSs), which represent idealised PSSs in the form of elliptical bodies with high aspect ratio. Previous workers have investigated the stress distributions around LVRSs with smooth flanks using a spring network model (Katsman et al., 2006), an anti-crack boundary element model (Sternlof et al., 2005) and an elliptical inclusion model (Rudnicki, 2007). They found that the normal stresses at the tips of the LVRS are compressive and much larger than the remote stresses, but are slightly reduced in comparison on the flanks. These results may help to explain the in-plane lateral growth of PSSs for a short distance and the interaction between neighbouring PSSs to enhance lateral linkage. However, based on these stress conditions alone, it is not possible to explain the widening and transverse coalescence of PSSs. The models of Zhou and Aydin (2010) incorporate asperities associated with the PSSs to show that the stress perturbations associated with these may propel the transverse growth and coalescence of PSSs. Such rough surfaces in real limestone samples have been described in detail (Schmittbuhl et al., 2004). The initiation of asperities that cause roughness are suggested to be due to geometrical (Gall et al., 1998), mechanical (Angheluta et al., 2008; Bonnetier et al., 2009), and/or chemical (Koehen et al., 2007) heterogeneities present within the rock, though the exact mechanism of localisation has not been satisfactorily constrained.

Note that we separate the mergers of neighbouring PSSs by use the terms 'linkage' for lateral mergers, and 'coalescence' for transverse mergers.

2. Geological setting

In this study the PSSs are found at a broad range of scales in coastal outcrops of the Devonian Gyleen Formation located southeast of the city of Cork, Ireland (Fig. 2). This is a fluvial unit and is comprised of alternating mudstones and cross-bedded sandstones deposited on a coastal plain (Sleeman and Pracht, 1994). The Gyleen Formation is largely composed of quartz, muscovite mica, clays, and minor amounts of magnetite and chlorite. The locations for observations presented in this contribution are a beach accessed through a private holiday centre (Loc. 1 in Fig.2a) and at the tip of Roaches Point at coastal outcrops near the lighthouse (Loc. 2 in Fig.2a). PSSs are also found in other clastic rock formations in County Clare, the tectonic significance of which will be discussed in a future paper.

As with time-equivalent rock units in the Ouachita belt of the Gulf of Mexico and the Alleghenian belt of the Appalachians, the Gyleen Formation was deformed in the late Carboniferous/early Permian Variscan Orogeny in response to a predominantly north-south compression producing an approximately east-west structural fabric as shown in the geological map and cross section (Fig. 2). An average tectonic shortening in the Cork region was estimated to be roughly 50% (Ford and Ferguson, 1985; Cooper et al., 1986). Elevated palaeo-temperatures of 250 °C derived from the vitrinite reflectance values of Upper Palaeozoic rocks near Kinsale (located 30 km south of Cork) have been documented and are thought to have been maintained until the cessation of Variscan folding (Clayton, 1989). These temperatures are indicative of burial depths of 5–7 km (Clayton, 1989) and potentially of higher heat-flow from hydrothermal activity (Corcoran and Clayton, 2001).

Though bed-parallel PSSs associated with burial stress exist, the bed-perpendicular PSSs due to tectonic compression are the most pervasive and are the focus of this study. These PSSs form sub-parallel to fold axes and remain generally at high-angle to bedding regardless of the dip of the beds, suggesting that a majority of them

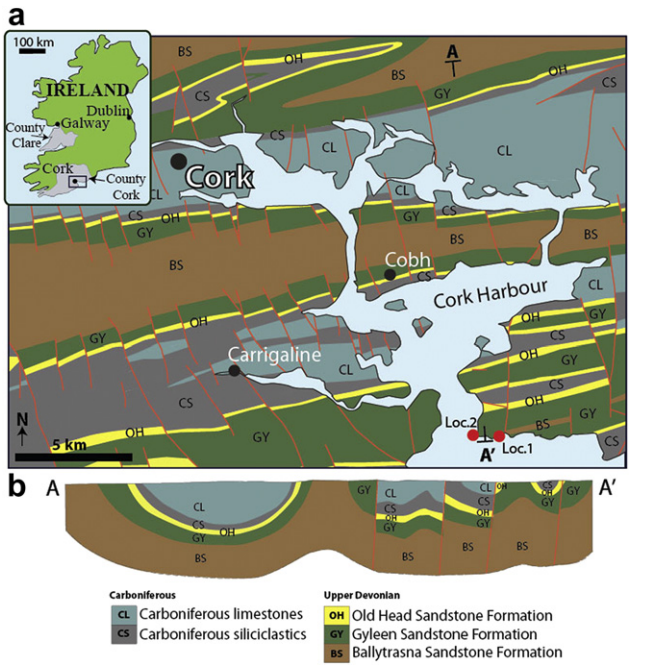

Fig. 2. Geological units and major fault and fold traces within County Cork, Ireland (a and inset) modified from Sleeman and Pracht (1994). Loc. 1 and Loc. 2 mark the locations of outcrops studied. A north-south cross-section shows the sub-surface geometry of the structures (b).

formed before folding took place. However, there is strong evidence for syn-folding or post-folding PSSs in the broader study area.

3. Methodology

We identified PSSs at high angle with respect to bedding and mapped them in the field on to low-level aerial photographs of outcrops, which were taken using a camera hoisted to an elevation of about 2.5 m using a pole. These photos were subsequently digitised and the PSS outlines were manually traced onto the images using Adobe Illustrator. The PSSs were identified macroscopically based on their colour (lighter than the matrix) and morphology (almost always with negative relief). We took hand samples containing seams (from locations 1 and 2 shown in Fig. 2) and cut and polished them for a clearer smooth surface on which to map. Mapping of the network of PSSs was accomplished by using enlarged digital images of the surfaces and tracing the outlines of PSSs manually using Illustrator. Again, the colour difference between the PSSs and the matrix was most useful in this mapping exercise. Next, we made thin sections oriented parallel to bedding for detailed analysis of PSSs at high angle to bedding using both optical and scanning electron microscopes. We used eighteen thin sections for optical microscopy, and six thin sections for electron microprobe analysis. The latter were imaged using a JEOL 733 electron microprobe in order to provide a qualitative characterisation of mineral abundance both in the relatively undeformed host rock and in the zones of PSSs within it. Secondary electron images (SEI) and backscatter electron images (BEI) were taken, the latter showing minerals containing heavier elements as higher intensity parts of the image. Electron dispersive spectroscopy was utilised to identify the composition of minerals and assign them to their respective intensity on the BEI. False colour images of the BEIs were created in order to gain a higher contrast image for visual differentiation between minerals. At this scale, the composition of the PSSs (high concentrations of clays and white mica) and location of quartz grain truncation were used to constrain the boundaries of the PSSs.

Using these images, we deciphered the constituent parts of PSSs at each scale of observation by graphically breaking down their complex geometries. Following this procedure, we reassemble these parts in the order responsible for the hierarchical evolution of PSSs. We also refer to an existing mechanical model to shed some light on the hypotheses and inferences regarding this growth process.

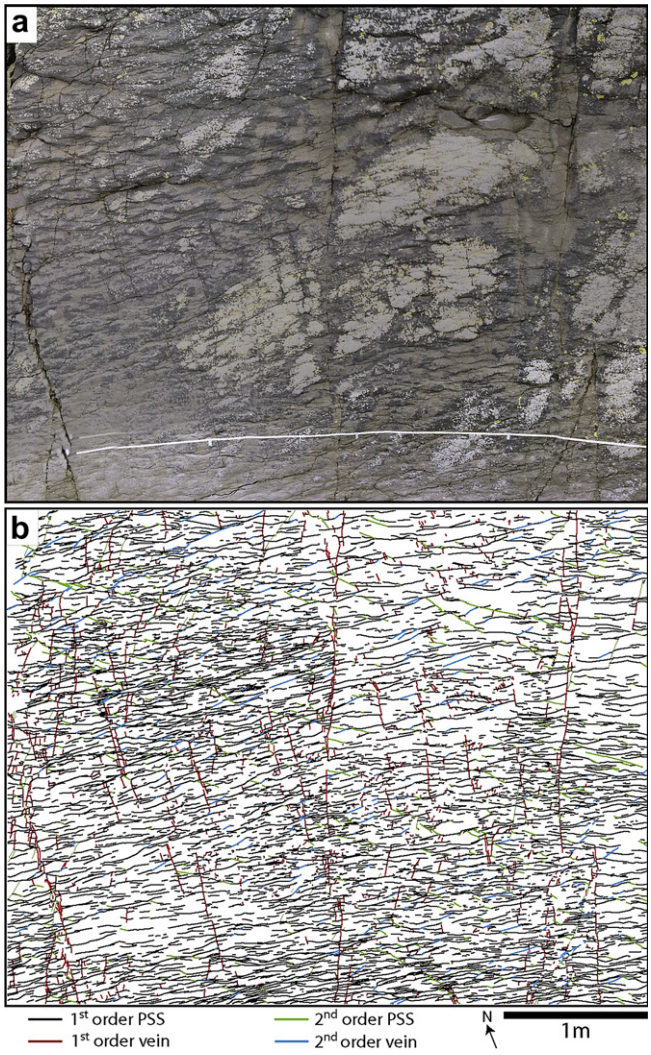

Fig. 3. A map view of the Gyleen Formation outcrop (for location see Fig. 2; loc 1). Photograph (a) and map (b) to show predominant 1st order bed-perpendicular PSS traces and 2nd order (splay) PSSs resulting from the shearing of the 1st order set. A few of the 1st order veins and 2nd order (splay) veins are also shown.

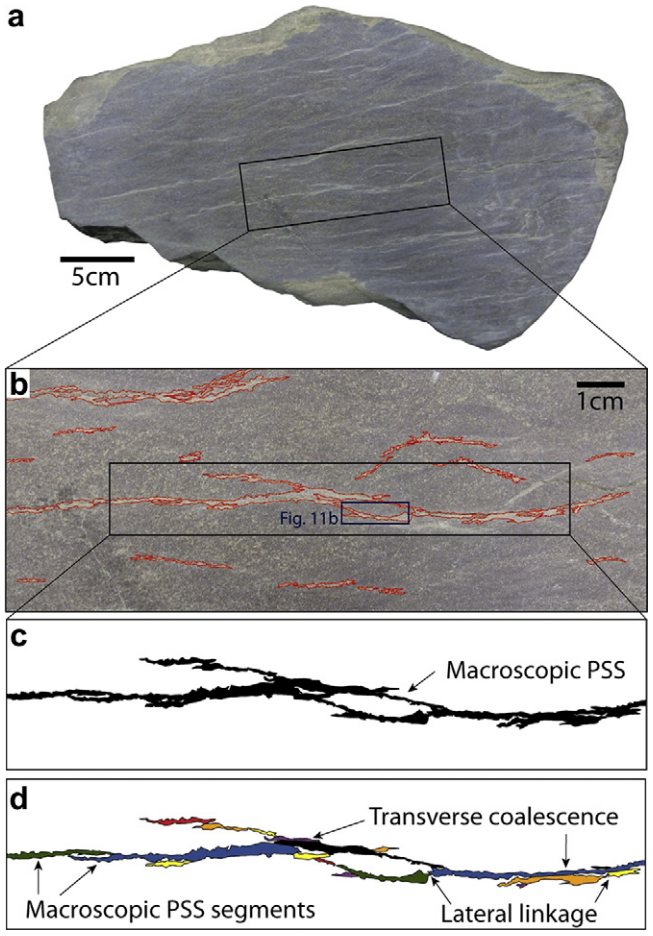

Fig. 4. Macroscopic pressure solution seams mapped on a polished surface of a hand sample from the Gyleen Formation (a and b), showing a complex PSS geometrical pattern (c). The interpretation of this pattern, in which the individual segments or strands are highlighted by different colours, is that neighbouring PSS segments have merged by lateral linkage and transverse coalescence (d). (For interpretation of the references to colour in this figure legend, the reader is referred to the web version of this article.)

4. Pressure solution seam characteristics

4.1. Macroscopic PSSs

Large macroscopic PSSs are observed at outcrops of the Gyleen Formation sandstone (Fig. 3). There are two sets of PSSs present: bed-parallel and bed-perpendicular. We focus on the latter, which are more dominant, parallel to local east-west fold axes and are therefore regarded as syntectonic in origin. The seams at outcrop scale have a sinuous form, and there is a colour contrast between the core of the seam and the surrounding material. The seams are preferentially eroded so that they have a negative relief relative to the rest of the outcrop.

In some places, the PSSs have been sheared to form 2nd order PSSs (splay PSSs) at an acute angle to the dominant set. Second order joints (splay joints), often filled as veins, at high-angle to the bed-perpendicular PSSs are also present in the rock. Neither of these 2nd order structures are a concern within this study.

Enlarged high-resolution images of polished hand sample surfaces show that the individual macroscopic PSSs are composed of smaller segments, which are sometimes isolated, but generally neighbouring segments are partially interconnected either laterally or transversely (Fig. 4). The individual segments were identified on the images by observing where the macroscopic seam has abrupt and irregular thickness changes and finger- or lobe-like dead ends that would be better explained as separate segments connected along parts of their flanks or at their tips. The segments are all in a similar orientation with respect to each other and to the macroscopic seam. Also, each mapped segment is thicker in its central parts and comes to a point at its tips in agreement with the observations of Stockdale (1922) amongst others.

4.2. Zones of incipient PSSs

Using an electron microprobe, we determined the composition of the rock both outside of, and within, the boundaries of macroscopic PSSs which were identified using their positions on the sample slab. The host rock is predominantly made up of quartz, clay material and some white mica (Fig. 5). The clay is mainly illite as determined by X-ray diffraction spectroscopy (Douglas McCarty,

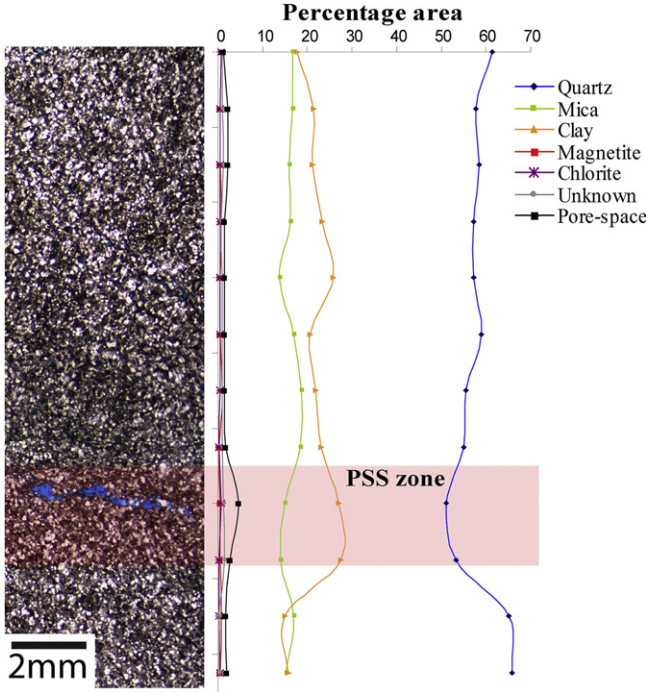

Fig. 5. Microprobe analysis of mineral proportions by area along a transect of a thin section that contains a zone of PSSs. Notice the decreasing percentage of quartz and mica and the increasing percentage of clay within the PSS zone. Blue epoxy fills a fracture within the PSS zone which post dates the dissolution process; the immediate area that includes the fracture itself was not included in the compositional analysis. However, the porosity increase around the fracture is likely due to the damage zone on the flank of the fracture. (For interpretation of the references to colour in this figure legend, the reader is referred to the web version of this article.)

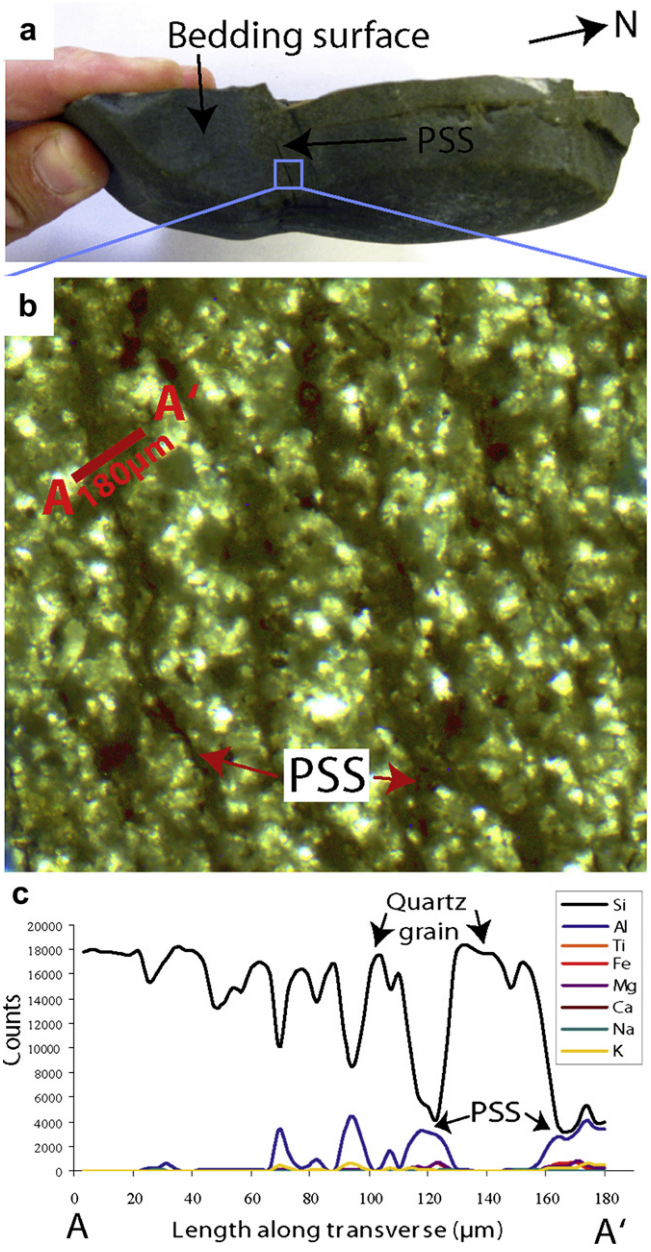

Fig. 6. Bedding perpendicular macroscopic PSS within a hand sample (a) from which a thick section was cut parallel to bedding containing bedding perpendicular incipient PSS (b). The blue areas are epoxy-filled pore spaces. Elemental analysis of a transverse through PSSs. X-ray counts recorded by wavelength dispersive spectroscopy across the transverse marked in (b) show aluminium-rich PSS whilst the host rock grains are predominantly composed of silica (c). (For interpretation of the references to colour in this figure legend, the reader is referred to the web version of this article.)

personal communication). The strain accommodated by this zone has been estimated by calculating the volumetric reduction of quartz due to dissolution, assuming that there is no significant amount of any other material being taken out of the system. Multiple backscatter electron images (each having an area of 0.64 mm^2 and spaced at 1.5 mm intervals) were taken along a scan line of the Gyleen Formation thin section containing a macroscopic PSS, with care not to take into account the area where the PSS has broken apart either during a younger deformation event or by the thin sectioning process. The amount of quartz within the PSS is 6.6% less than the average amount from the surrounding host rock, whereas the percentage of clay is 5.9% more in the zone as it remains after quartz grains have dissolved.

A qualitative chemical analysis of a macroscopic PSS using wavelength dispersive X-ray spectroscopy shows that the seam has a relative abundance of aluminium, iron and potassium compared to the silica which forms the bulk of the host rock (Fig. 6). A single macroscopic PSS observed in the thin section image contains numerous clay-rich smaller PSSs identified by wavelength dispersive X-ray spectroscopy. In the 180 μm long transverse analysed, several longer solution seams are present along with many short, poorly developed seams at this scale.

We term these microscopic seams as incipient PSSs, and they localise in approximately 100–600 μm thick zones that make up the macroscopically identifiable seams (Figs. 7 and 8). These are probably what have previously been considered as a single lamina of residue at the core of a macroscopic PSS (Stockdale, 1922; Buxton and Sibley, 1981; Andrews and Railsback, 1997). Incipient PSSs are also present outside of the zone in the host rock, but these cannot be seen with the naked eye.

4.3. Individual incipient PSSs

The individual incipient PSSs can be positively identified using an SEM and are defined as a relatively thick (~2 μm) band of clay and white mica which remain as the residual minerals between the truncated quartz grains (Fig. 9). These seams involve a few neighbouring grain boundaries that are truncated at the grain to grain contact. Quartz grains that are still present within the seam are much smaller in size than those outside. Incipient PSSs have a consistent orientation and are pervasive throughout the sample.

4.4. Inter-granular PSSs between 2 quartz grains

Using SEM images, the incipient PSSs can be observed in juvenile stages as isolated dissolution between only two quartz grains.

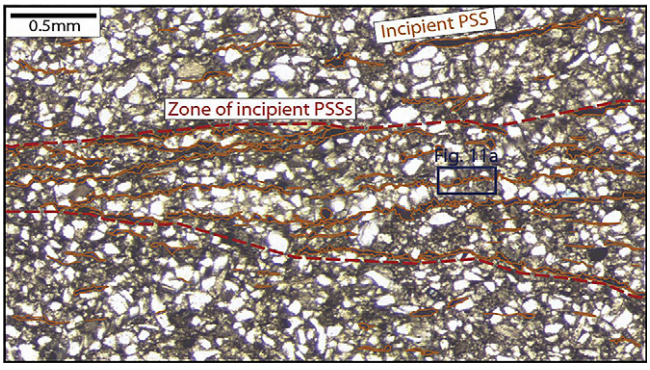

Fig. 7. Plane-polarized thin section image showing a zone of incipient microscopic PSSs. Zones such as this constitute the macroscopic PSSs that can be observed by eye in hand specimen-scale samples.

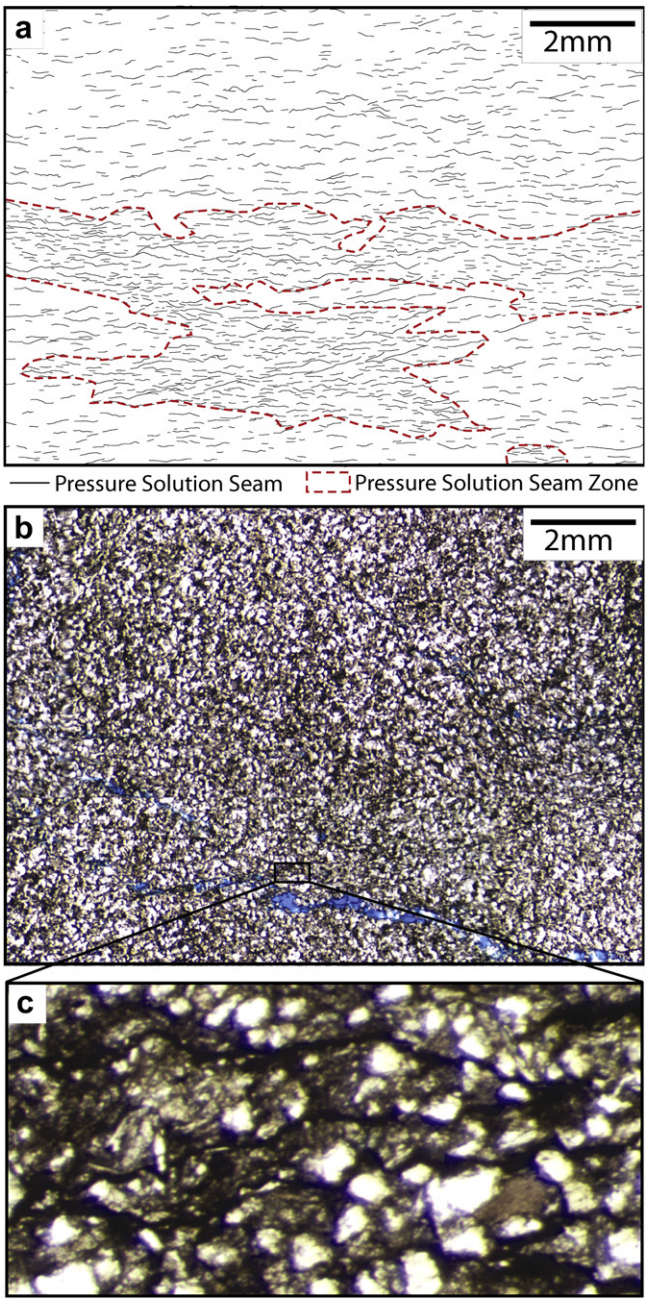

Fig. 8. Map showing a zone of incipient PSSs (a) from a plane-polarized bedding-parallel oriented thin section image (b). A magnified portion of the thin section shows the dark colour and geometry of the incipient PSSs; these characteristics were used as the basis for mapping the PSS boundaries (c).

These are inter-granular PSSs, and are defined by aligned pockets of insoluble clay (illite) and white mica along boundaries between neighbouring quartz grains (Fig. 10a). Dissolution is not only in orientations corresponding to the macroscopically identified PSSs, though these seams are particularly well developed, but can be observed at most quartz grain to grain boundaries.

Estimating strain across truncated grain to grain contacts due to dissolution can be accomplished by calculating the percentage shortening between the projected original grain shapes and the current position of the interpenetrated grains (Onasch, 1993). Using this method for 14 interpenetrating grain pairs in 3 thin sections, average shortening was determined to be approximately 20%. The

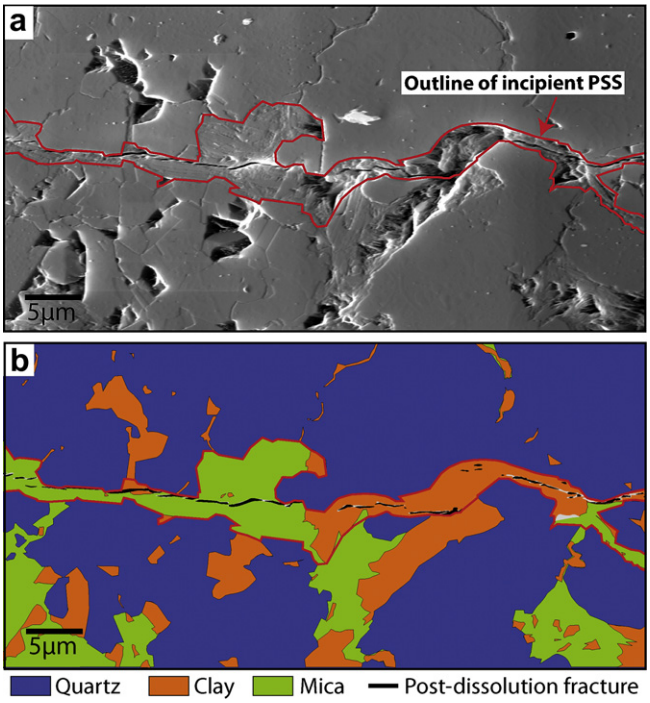

Fig. 9. Secondary electron image (a) and false colour image (b) of a through going incipient single PSS at high magnification. The seam is identified as a mica- and clay-rich core between multiple truncated quartz grains. Segmented open fractures along the zone are due to a younger deformation phase or thin sectioning. Note the irregular boundaries due to the mergers of lobes of undissolved material to the linear PSS.

maximum strain calculated is 37.7%. In this process, it is assumed that the grains were originally ellipsoid in shape, that they were displaced as rigid bodies, and that the shortening occurs in an orientation parallel to the tie-line that links the centre points of the two grains. To cater for the latter point, the measurements were only taken where the tie-line orientation was sub-perpendicular to the general PSS orientation. Fig. 10b shows an example secondary electron image of 3 quartz grains used for strain estimation with the assumed original ellipsoid grain boundaries mapped for reference. Note that the estimated strain is likely to be a minimum value since the estimated ellipsoid may have been more oblate.

4.5. Pressure solution seam roughness

The boundaries of PSSs are irregular at all scales of observation (as seen in Figs. 5–10). The first order roughness is at the grain scale, where the quartz grain boundaries have some roughness and isolate sites of dissolution and pockets of clays and micas (Fig. 10a). As a PSS grows and incorporates multiple grains, the geometry of the grains adjacent to the seam and the interstitial space between these grains contribute to the second order roughness of the PSS boundary (Fig. 9). Third order roughness is created in the form of asperities observable at the hand-sample scale where seams link due to lateral growth and transverse coalescence to form zones of compound PSSs (Fig. 4). The geometry of asperities that form the irregularities on the flanks of PSSs is variable. The most common asperity shapes mapped in thin section and hand sample images of PSSs (Fig. 11) can be approximated as rectangular, semi-circular and triangular which some authors have referred to as a 'conical' geometry (Gratier et al., 2005). The presence of seam roughness has implications for the local stresses around the PSSs and their thickening mechanism as will be analysed later in this paper.

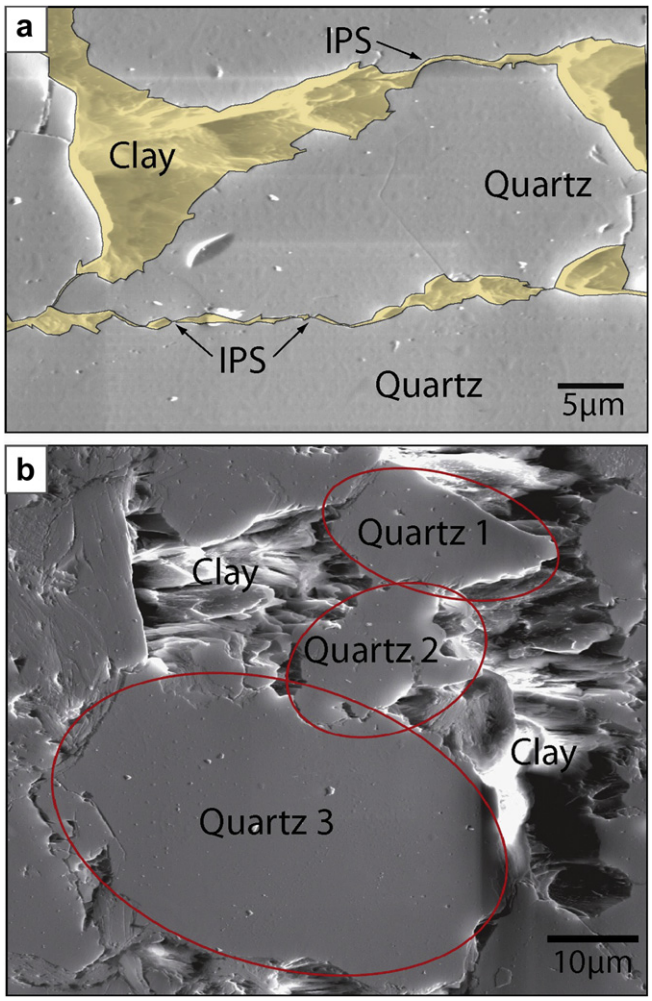

Fig. 10. Secondary electron images to show the initial stage of inter-granular pressure solution (IPS) which can be identified by isolated pockets of clay between two inter-penetrating quartz grains (a) and the assumed original boundaries of quartz grains used to estimate strain associated with dissolution (b).

4.6. Pressure solution seam thickness-length relationship

As a separate study, we investigated the statistical properties of PSSs in clastic rocks and compared them with those of opening mode joints. A part of this study involved measuring the lengths and thicknesses of PSSs at outcrop (Fig. 3), in hand sample (Fig. 4) and in thin section (Fig. 8). This plot indicates that PSSs grow proportionally in length, L, and thickness, T, with the power-law relationship $T = 0.013L^{0.70}$ within the observed range of scales (Fig. 12). The gap in the data represents measurements that are below the resolution of images taken of the hand sample, but above that of the thin section images.

We envision that the growth happens in a systematic manner as depicted in our conceptual model below.

5. Conceptual model

We have presented PSS observations from outcrop to grain scale due to the advantage of identifying the structures in subsequently smaller scales. However, it is more informative, in terms of growth of a single PSS, to change the order by reassembling the parts that we have already identified in the previous sections. In this way, the mechanisms responsible for growth of PSSs from a simple

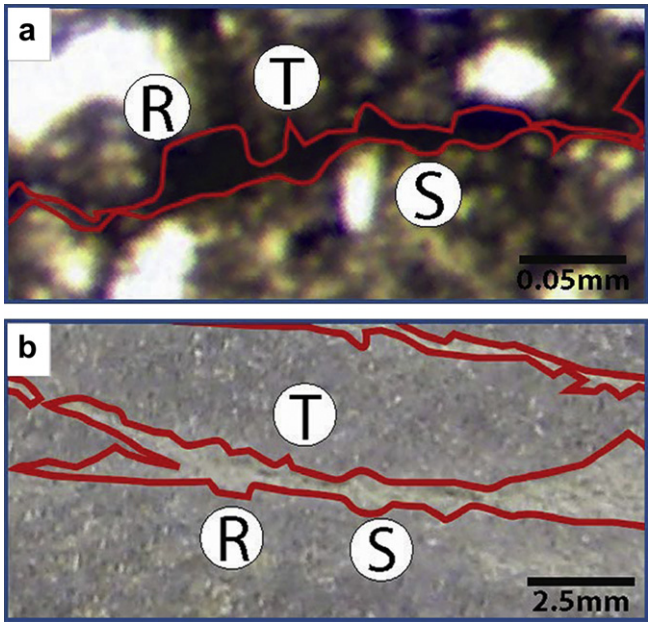

Fig. 11. Irregular PSS boundaries can be approximated as rectangular (R), triangular (T), or semi-circular (S) at thin section (a) and hand sample (b) scales. These images have been enlarged from the blue boxes in Figs. 4 and 7 respectively.

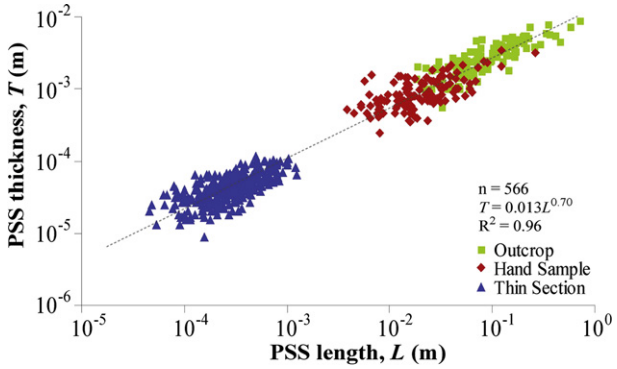

Fig. 12. A log–log plot to show the power-law relationship between PSS length and thickness measured from outcrop, hand sample and thin section maps.

inter-granular PSS between two grains in contact, to a mature macroscopically identifiable structure can be appreciated (Fig. 13).

Under a compressive normal stress, the mechanical dissolution of two quartz grains along their mutual interface forms inter-granular PSSs with the aid of the assumed presence of a fluid film (Fig. 13a). This tendency may be enhanced by the presence of brine and pre-existing clays or micas between the quartz grains. Clays and micas remaining after the quartz grains have dissolved act to thicken the layer of aligned insoluble material at the core (see Stockdale, 1922; Sarfaricz and Davison, 2005; Hassan, 2007), that is, allowing transverse growth of the seam.

The individual inter-granular PSSs may propagate laterally in-plane for a short distance and link with the neighbouring PSSs, resulting in a longer compound structure which we term incipient PSSs (Figs. 13b and 14). Similarly, transverse coalescence occurs where the dissolvable material between the two existing seams is removed completely so that the transversely overlapping seams are merged into a thicker coalesced seam (Fig. 14b). The linkage of the PSS boundaries may create additional roughness along the flanks of the resulting compound structure (Fig. 14c). Such a compound PSS was also reported by Chanchani et al. (1996) without identifying the mechanism responsible for the structure.

The next stage of PSS evolution is a zone made up of numerous short incipient PSSs that are closely spaced (Fig. 13c). This appears as a single macroscopic structure (Fig. 13d) which may continue to grow by lateral in-plane linkage and transverse coalescence allowing smaller seams to converge into longer and thicker seams (Figs. 3b and 4a).

The effects of seam roughness and the geometry of asperities on local compressive stresses on the flanks of PSSs have been evaluated by Zhou and Aydin (2010), and we here introduce some of their major findings in order to justify the inferred PSSs lengthening and thickening process.

6. Mechanical bases for the growth of pressure solution seams

Previous studies have modelled PSSs or their mathematical counterparts, LVRSs, as elliptical inclusions with high aspect ratios (Zhou and Aydin, 2010; Aharonov and Katsman, 2009; Katsman et al., 2006; Sternlof et al., 2005) under compressive loading conditions. For example, the distribution of the local normal stresses around an elliptical LVRS normalised by the remote stress perpendicular to the LVRS, $\sigma_{yy}/\sigma^{r}_{yy}$, is shown in Fig. 15a. All these studies showed a significant compressive stress concentration at the lateral tip of the LVRS, which was used to rationalise lateral propagation of PSSs to increase their lengths and to laterally link with the neighbouring segments or strands. These studies have also pointed out that the normal stresses on the flanks of the LVRSs with smooth interfaces are reduced with respect to the remote stress normal to the structure (Fig. 15a). Hence, the modelling results show that the LVRSs with smooth flanks may be able to grow laterally in-plane for some distance and to link laterally with adjacent structures nearby. However, based on these stress conditions alone, it is not possible to explain the widening and transverse coalescence of PSSs.

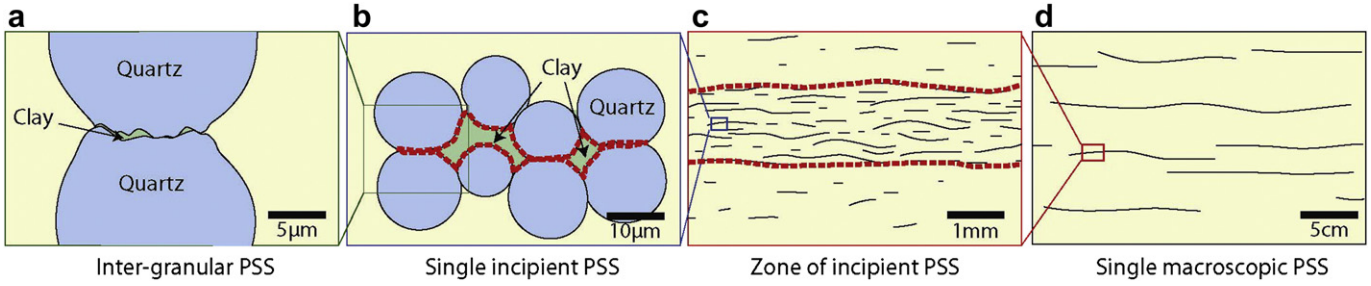

Fig. 13. Summary of the conceptual evolution of pressure solution seams. The smallest observed structures are inter-granular PSSs (a). Growth and linkage of adjacent inter-granular PSSs form incipient PSSs involving multiple grain boundaries (b). Incipient PSSs grow by in-plane propagation, lateral linkage and transverse coalescence. These seams concentrate in zones (c) that are visible in hand samples as single macroscopic PSSs (d).

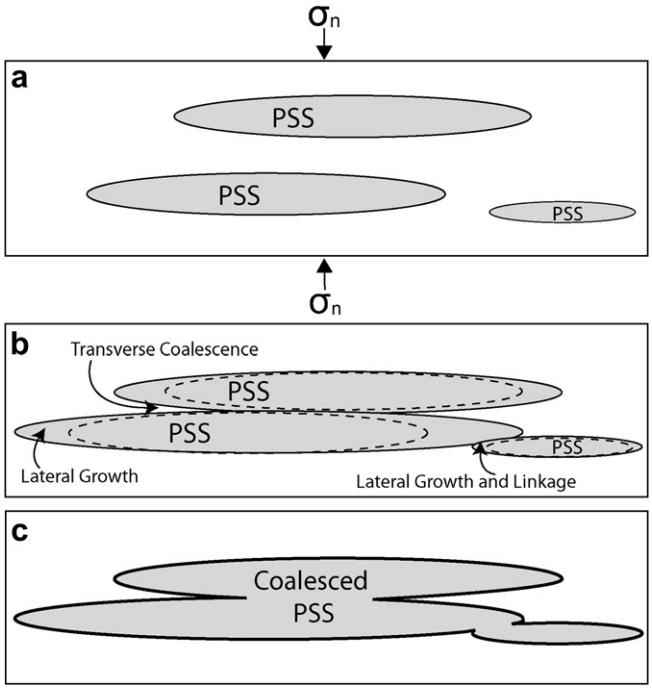

Fig. 14. Idealised array of PSSs within a rock subjected to compressive stresses (a) may grow in thickness due to transverse coalescence, and in length due to lateral in-plane propagation and linkage with neighbouring PSS segments (b). Outline of the compound PSS or PSS zone illustrating the notion that increased roughness may be caused by the lateral linkage of neighbouring PSS segments (c). Note the finger- and lobe-like extensions resulting from the mergers.

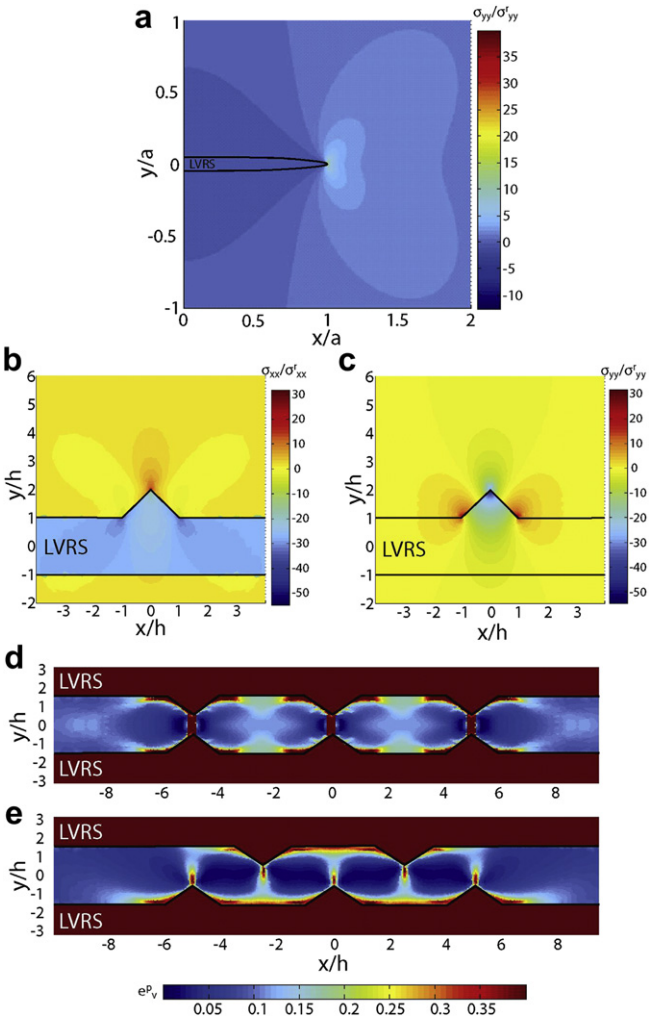

Fig. 15. Numerical model results from Zhou and Aydin (2010) to show the σ_{yy} contours, normalised by the remote stress σ^{r}_{yy} around an elliptical LVRS with aspect ratio of 20 (a). Here it is assumed that $e^{p}_{xx} = 0$, $E = 20$ GPa, $\nu = 0.25$, $\sigma^{r}_{yy} = 100$ MPa. The compressive normal stress concentrations occur at the tip areas. However, σ_{yy} decreases on the flanks of the LVRS compared to the remote stress; the normalised stress distributions around the triangular asperities due to both the initial plastic strains within the LVRS ($e^{p}_{xx} = 0.1$, $e^{p}_{yy} = 0.3$) and the remote bi-axial stress loadings ($\sigma^{r}_{xx} = 75$ MPA, $\sigma^{r}_{yy} = 100$ MPa) (b and c). The concentrations of σ_{xx} at the top (b) and σ_{yy} at the base (c) of the triangular asperities can be observed; and distributions of volumetric plastic strains, e^{p}_{v}, between two parallel and perfectly symmetric (d) and asymmetric (e) LVRSs with triangular asperities on the flanks after 1000 years of deformation. The spacing between the flanks of the two LVRSs is $s = 3h$, where h is the height of the triangular asperities. The case with symmetric asperities facilitates a stronger interaction between two parallel overlapping LVRSs.

Motivated by the observations presented in this present paper, Zhou and Aydin (2010) have modelled LVRSs with rough flank geometry to test a hypothesis that the roughness may result in an increasing stress concentration locally at an LVRS's flanks thereby inducing PSSs lateral growth. They have idealised the flank asperities as triangular, rectangular, and semi-circular in a finite element model. Fig. 15b and c show the normalised stress distributions around the triangular asperities due to both an initial plastic strain within the LVRS ($e^{p}_{xx} = 0.1$, $e^{p}_{yy} = 0.3$) and the remote bi-axial stress loading ($\sigma^{r}_{xx} = 75$ MPa, $\sigma^{r}_{yy} = 100$ MPa). The concentrations of stresses in *x*-direction ($\sigma_{\mathbf{xx}}$) at the top (Fig. 15b), and *y*-direction ($\sigma_{\mathbf{yy}}$) at the base (Fig. 15c), of the triangular asperity are seen. The same authors also investigated the distribution of volumetric plastic strains between two parallel and perfectly symmetric (Fig. 15d) and asymmetric (Fig. 15e) LVRSs with triangular asperities on the facing flanks after 1000 years of deformation using a creep law. The spacing between the flanks of the two parallel LVRSs is three times of the height of the triangular asperities. In both cases there are high volumetric plastic strain concentrations at the base and the tips of the triangular asperities but the case with symmetric asperities along facing flanks of neighbouring PSS strands facilitates a stronger interaction and consequently higher volumetric plastic strains.

Zhou and Aydin (2010) concluded that the results for rectangular and semi-circular asperities are similar to those for the triangular ones reported here. These results substantiate the proposed transverse growth and coalescence mechanisms inferred from our field and microscopy studies.

7. Discussion

We have described PSSs in low porosity clastic rock and have mapped them in increasing detail in order to identify their constituent parts. We then reassembled these parts together to elucidate the initiation and the growth of PSSs as a hierarchy of segment and strand linkage and coalescence processes. Figs. 13 and 14 are conceptual diagrams showing these progressive stages: growth and linkage of adjacent inter-granular PSSs form incipient PSSs involving multiple grain boundaries (13a), Incipient PSSs grow by in-plane propagation and progressive lateral linkage and transverse coalescence (13b). These seams concentrate in zones (13c) that are visible in hand samples as single macroscopic PSSs (13d). Termination of the insipient single PSS at its tip may be due to propagation into a mineral more resistant to dissolution or a quartz grain in an unfavourable crystallographic orientation in the location through which PSS segments may have otherwise continued to link together. The thickness versus length plot of the

PSS at various hierarchical scales (Fig. 12) further supports our interpretations that the PSSs thicken and widen as they evolve.

Thickening of pressure solution seams by transverse coalescence was suggested as a growth mechanism by many including Stockdale (1922) and Oelkers et al. (1996). These authors noted that, as quartz dissolves, not only does the distance between seams decrease until they ultimately merge, but any detrital clays and heavy minerals between the seams also accumulate which adds to the combined seam thickness. Our results support these notions. The FEM results presented by Zhou and Aydin (2010) provide a foundation for how this transverse growth in particular is feasable and reinforce the interpretations made for PSS growth mechanisms.

Individual stages of pressure solution evolution have, of course, been described in previous works generally within the context of experimentally produced PSSs (Martin et al., 1999; Gratier et al., 2005; Rossi et al., 2007), naturally produced PSSs at only a narrow scale range of observation (Peacock and Sanderson, 1995; Andrews and Railsback, 1997; Graham Wall et al., 2006), or without explanation of how smaller PSSs link to form their larger scale counterparts (Helmstaet and Greggs, 1980; Hassan, 2007). At small scales, PSS features such as grain truncation have been observed by many previous investigators (for example, Onasch, 1994), and it is suggested that cements are likely sourced from the dissolved material (Oelkers et al., 1996; Gratier et al., 1999; Baron and Parnell, 2007; Van Noort and Spiers, 2009). Unlike studies within limestones, there are few studies reporting decimetre scale observations of PSSs within clastic rocks. PSSs within limestones are often observed to have sutured tooth-like geometries as noted earlier (Stockdale, 1922; Baron and Parnell, 2007; Fabricius and Borre, 2007; Hassan, 2007), but such geometries are not common within the clastic rocks of this study. Instead, the trace geometries of PSSs appear to be wavy, curvi-linear and crooked with finger- or lobe-like extensions along their lengths. In some places they have sharp triangular asperities on their flanks.

A possible causative effect is the presence of the clays and micas which act to increase the rate of quartz dissolution where present (Heald, 1959; Weyl, 1959; Dewers and Ortoleva, 1991; Hickman and Evans, 1995; Rutter and Wanten, 2000; Rossi et al., 2007; Aharonov and Katsman, 2009). A suggested reason is that phylosillicate films between clean quartz grains form multiple sheeted fluid pathways to allow a greater rate of diffusion than a single absorbed water film on a quartz surface would allow, provided the micas are less prone to pressure solution than the quartz grains (Weyl, 1959). Some authors have suggested that clays must be present in order for pressure solution to occur at all, presumably having observed no evidence of cement sourced from purely quartz–quartz interfaces within sandstones (Oelkers et al., 1996). However, experimental results indicate that the presence of clays is not a prerequisite for pressure solution occurrence (Rossi et al., 2007).

In this study, the likelihood that the clay-bearing seams are a depositional phenomenon rather than due to physico-chemical processes is not supported as the observed seams are elongate in form and are oriented sub-perpendicular to bedding planes and parallel to local fold axes. It may be that some of the clays were present as elongate grains in the host rock independent of pressure solution processes or that the grains were not originally elongate and were reshaped due to the applied compressive stresses. However, while the provenance of the clay material within PSSs may be debatable, their role in PSS evolution and growth is no different.

Previous studies rationalised the lateral progression of PSSs (or their mathematical counterparts, LVRSs or anticracks) based on the stress concentration at the tips (Zhou and Aydin, 2010; Aharonov and Katsman, 2009; Katsman et al., 2006; Sternlof et al., 2005). Further, these authors showed that compressive stresses decrease on the flanks of LVRSs. Sternlof (2006) suggested that anticracks (which crudely represent PSSs) maintain an elliptical shape as they propagate, meaning that the bands thicken as they grow in length. However, it is difficult to explain thickening because of the diminished normal compressive stresses on the flanks. Thickening of PSSs through transverse coalescence has not been adequately explained in the literature. In this study, we hypothesise that the roughness of PSS surfaces may be responsible for additional stress concentration at the flanks of LVRSs thereby facilitating the transverse growth of the LVRSs.

Asperities on the flanks of PSSs at all of the observed scales may be idealised as either triangular, semi-circular, or rectangular shape (Fig. 11). Bernabe and Evans (2007) and Bernabe et al. (2009) numerically modelled the compression of circular asperities against a flat surface. Zhou and Aydin (2010) considered geometric irregularities on the flanks of their LVRS model. Their mechanical analyses show that the asperities in the form of triangles, rectangles or semi-circles are capable of producing significant stress perturbations along the flanks of the LVRSs. This suggests, based on the stress contribution alone, that surface roughness may facilitate the growth of asperities, thereby resulting in wider LVRSs and resulting in transverse coalescence of neighbouring structures.

Macroscopic PSSs in Albanian limestones studied by Graham Wall et al. (2006) were described to have amplitudes 'from millimetres to centimetres'. Similarly, Baron and Parnell (2007) state amplitudes of between 0.1 and 1 cm for PSS within limestones from Scotland and Greenland. Although stylolite amplitude is not necessarily a direct function of strain (Koehn et al., 2007), it may provide a minimum value for shortening across the seam (Stockdale, 1922). The asperity shapes of these stylolites can in most cases be approximated as rectangular and triangular. From limestone examples, PSS roughness has been described in terms of stylolite amplitude or roughness (Renard et al., 2004; Brouste et al., 2007; Koehn et al., 2007; Ebner et al., 2009). Renard et al. (2004) demonstrated that the roughness of stylolites from limestone samples has self-affine behaviour that falls into two regimes separated by a well-defined characteristic length. The presence of roughness over a wide range of scales is consistent with our notions for PSSs in clastic rock seven though we have not characterised the PSS roughness statistically. Roughness of PSSs in limestones is thought to be generated from differential dissolution rates along the seam (Guzzetta, 1984) and also may be a function of grain size (Ebner et al., 2009).

In the clastic material of this study, at the smallest observed scale, roughness is a result of not only differential dissolution, but also of grain boundary geometry so that the incipient PSSs have amplitudes that are dependant on grain size and distribution. Furthermore, the amplitude of PSSs increases with scale of observation due to the out of plane linkage of its constituent segments (Figs. 4,8–10). Macroscopic PSSs observed in the polished hand sample from the Gyleen formation are sinuous or crooked rather than having stylolitic teeth as seen in limestones, and have amplitudes in the order of 0.5 cm (Fig. 3). In all scales of observation, PSSs have finger- or lobe-like dead ends which we attribute to the fundamental process of the PSS's growth as idealised in Fig. 14. Hence the roughness of PSSs crosses over scales even though its mathematical form may vary with length (Renard et al., 2004).

8. Conclusions

PSSs as seen in outcrop in clastic rocks are complex structures which are formed by a hierarchy of linked and merged segments and strands. We document geometries of PSSs at many scales showing that the seams initiate as poorly-organised inter-granular pressure solution seams at quartz grain to grain contacts where

clays or muscovite mica may be present to a certain extent. The seams grow in length by in-plane growth and linkage of adjacent segments, and in thickness by transverse coalescence of overlapping individual seams. Less soluble minerals are brought to the core of the seam as quartz is dissolved and removed from the system. Growth and linkage of aligned or closely spaced en echelon adjacent inter-granular PSSs form incipient PSSs which have a consistent orientation and involve multiple grain boundaries. Transverse growth occurs by dissolution along the flanks and eventually by coalescence of neighbouring sub-parallel features due to the removal of the entire strings of the load-bearing quartz grains.

Multiple incipient PSSs can concentrate in thin tabular zones that are visible to the eye in hand specimens. At this scale, the zones act as single macroscopic PSSs that may further coalesce by lateral or transverse linkage to lengthen and thicken the seams respectively. The ultimate length of a seam may be limited by the dissipative tendency of the plastic tip strains, the presence of less soluble minerals in the potential propagation path of the seam or by the presence of orthogonal structures such as other seams, joints or veins.

Our concepts are substantiated by the most recent mechanical models of Zhou and Aydin (2010) among others. They show that the normal stresses at the tips of smooth elliptical LVRSs are compressive and significantly amplified relative to the background values, whereas they are reduced on the flanks. These stress perturbations may be used to rationalise the in-plane growth of the PSSs. The mechanical analyses for LVRSs with various geometric asperities (triangular among others) on their flanks are based on the laboratory and field observations that the PSS surfaces are extremely rough. These asperities can induce significant increase in the compressive normal stresses and volumetric plastic strains around the asperities compared to the remote values. Therefore, the presence of asperities indicates a greater potential for the transverse growth and coalescence of PSSs.

Acknowledgements

Thanks go to Xiaoxian Zhou for his contributions and discussions concerning the numerical modelling of LVRSs; to Gareth Seward (University of California, Santa Barbara) and Bob Jones (Stanford University) for their guidance and expertise with regard to the microprobe analysis; and to Eric Flodin and Douglas McCarty at Chevron for their XRD analysis of one sample. Thanks also go to two anonymous reviewers for their suggestions about the original manuscript. We are grateful for the funding received for this study through a Levorsen grant from Stanford University, partial fieldwork funding from the Stanford Department of Earth and Environmental Sciences and through the Stanford Rock Fracture Project.

References

Agosta, F., Aydin, A., 2006. Architecture and deformation mechanism of a basin-bounding normal fault in Mesozoic platform carbonates, central Italy. Journal of Structural Geology 28, 1445–1467.

Aharonov, E., Katsman, R., 2009. Interaction between pressure solution and clays in stylolite development: insights from modelling. American Journal of Science 309, 607–632.

Andrews, L.M., Railsback, L.B., 1997. Controls on stylolite development: morphologic, lithologic and temporal evidence from bedding parallel and transverse stylolites from the U.S. Appalachians. The Journal of Geology 105, 59–73.

Angheluta, L., Jettestuen, E., Mathiensen, J., Renard, F., Jamtveit, B., 2008. Stress driven phase transformation and the roughening of solid-solid interfaces. Physical Review Letters 100, 096105.

Baron, M., Parnell, J., 2007. Relationships between stylolites and cementation in sandstone reservoirs: examples from the north Sea, U.K. and east Greenland. Sedimentary Geology 194, 17–35.

Bathurst, R.G.C., 1995. Burial diagenesis of limestones under simple overburden. Stylolites, cementation and feedback. Société Géologique de France, Bulletin 166, 181–192.

Bernabe, Y., Evans, B., 2007. Numerical modelling of pressure solution deformation at axisymmetric asperities under normal load. In: David, C., Le Ravalec-Dupin, M. (Eds.), Rock Physics and Geomechanics in the Study of Reservoirs and Repositories. Geological Society of London, Special Publication, 284, pp. 185–205.

Bernabe, Y., Evans, B., Fitzenz, D.D., 2009. Stress transfer during pressure solution compression of rigidly coupled axisymmetric asperities pressed against a flat semi-infinite solid. Pure and Applied Geophysics 166, 899–925.

Bjørlykke, K., Egeberg, P.K., 1995. Quartz cementation in sedimentary basins. The American Association of Petroleum Geologists Bulletin 77, 1538–1548.

Bonnetier, E., Misbah, C., Renard, F., Toussaint, R., Gratier, J.-P., 2009. Does roughening of rock-fluid-rock interfaces emerge from a stressed-induced instability? The European Physical Journal 67, 121–131.

Brouste, A., Renard, F., Gratier, J.-P., Schmittbuhl, J., 2007. Variety of stylolites' morphologies and statistical characterization of the amount of heterogeneities in the rock. Journal of Structural Geology 29, 422–434.

Buxton, T.M., Sibley, D.F., 1981. Pressure solution features in a shallow buried limestone. Journal of Sedimentary Petrology 51, 19–26.

Carrio-Schaffhauser, E., Raynaud, S., Latiere, H.J., Mazerolle, F., 1990. Propagation and Localization of Stylolites in Limestones, Deformation Mechanisms, Rheology and Tectonics. In: Geological Society Special Publication, 54, 193–199.

Chanchani, J., Berg, R.R., Lee, C., 1996. Pressure solution and microfracturing in primary oil migration, Upper Cretaceous Austin Chalk, TexasGulf coast. Transactions of the Gulf Coast Association of Geological Societies 46, 71–78.

Clayton, G., 1989. Vitrinite reflectance data from the Kinsale Harbour-Old Head of Kinsale area, southern Ireland, and its bearing on the interpretation of the Munster basin. Journal of the Geological Society, London 146, 611–616.

Cooper, M.A., Collins, D.A., Ford, M., Murphy, F.X., Trayner, P.M., O'Sullivan, M., 1986. Structural evolution of the Irish Variscades. Journal of the Geological Society, London 143, 53–61.

Corcoran, D.V., Clayton, G., 2001. Interpretation of Vitrinite Reflectance Profiles in Sedimentary Basins, Onshore and Offshore Ireland. In: Geological Society, London, Special Publications, 188, 61–90.

Dewers, T., Ortoleva, P., 1991. Influences of clay minerals on sandstone cementation and pressure solution. Geology 19, 1045–1048.

Dunnington, H.V., 1967. Stylolite development post-dates rock induration. Journal of Sedimentary Petrology 24, 27–49.

Ebner, M., Koehn, D., Toussaint, T., Renard, F., 2009. The influence of rock heterogeneity on the scaling properties of simulated and natural stylolites. Journal of Structural Geology 31, 72–82.

Fabricius, I.L., Borre, M.K., 2007. Stylolites, porosity, depositional texture, and silicates in chalk facies sediments, Ontong Java Plateau - Gorm and Tyra fields, North Sea. Sedimentology 54, 183–205.

Fletcher, R.C., Pollard, D.D., 1981. Anticrack model for pressure solution surfaces. Geology 9, 419–424.

Ford, M., Ferguson, C.C., 1985. Cleavage strain in the Variscan fold belt, County Cork, Ireland, estimated from stretched arsenopyrite rosettes. Journal of Structural Geology 7, 217–223.

Gall, D., Nur, A., Aharonov, E., 1998. Stability analysis of a pressure solution surface. Geophysical Research Letters 25, 1237–1240.

Graham Wall, B.R., Girbacea, R., Mesonjesi, A., Aydin, A., 2006. Evolution of fracture and fault-controlled fluid pathways in carbonates of the Albanides fold-thrust belt. American Association of Petroleum Geologists Bulletin 90, 1227–1249.

Gratier, J.-P., Renard, F., Labaume, P., 1999. How pressure solution creep and fracturing processes interact in the upper crust to make it behave in both a brittle and viscous manner. Journal of Structural Geology 21, 1189–1197.

Gratier, J.-P., Muquet, L., Hassani, R., Renard, F., 2005. Experimental microstylolites in quartz and modelled application to natural stylolitic structures. Journal of Structural Geology 27, 89–100.

Gratier, J.-P., Guiguet, R., Renard, F., Jenatton, L., Bernard, D., 2009. A pressure solution creep law or quarts from indentation experiments. Journal of Geophysical Research 114, B03403. 10.029/2008JB005652.

Groshong, R.H., 1988. Low-temperature deformation mechanisms and their interpretation. Geological Society of America Bulletin 100, 1329–1360.

Guzzetta, G., 1984. Kinematics of stylolite formation and the physics of the pressure-solution process. Tectonophysics 101, 383–394.

Hassan, H.M., 2007. Stylolite effect on geochemistry, porosity and permeability: comparison between a limestone and a dolomite sample from Khuff-B reservoir in eastern Saudi Arabia. Arabian J. for Sci. Eng. 32, 139–148.

Heald, M.T., 1959. Significance of stylolites in permeable sandstones. Journal of Sedimentary Petrology 29, 251–253.

Helmstaet, H., Greggs, R.G., 1980. Stylolitic cleavage and cleavage refraction in lower Paleozoic carbonate rocks of The Great Valley, Maryland. Tectonophysics 66, 99–114.

Hickman, S.H., Evans, B., 1995. Kinetics of pressure solution at halite-silica interfaces and intergranular clay films. Journal of Geophysical Research 100, 13113–13132.

Katsman, R., Aharonov, E., Scher, H., 2006. A numerical study on localized volume reduction in elastic media: some insights on the mechanics of anticracks. Journal of Geophysical Research 111, B03204. doi:10.1029/2004JB003607.

Koehn, D., Malthe-Sorenssen, A., Passchier, C.W., 2006. The structure of reactive grain boundaries under stress containing confined fluids. Chemical Geology 230, 207–219.

Koehn, D., Renard, F., Toussaint, R., Passchier, C.W., 2007. Growth of stylolite teeth patterns depending on normal stress and finite compaction. Earth and Planetary Science Letters 257, 582–595.
Lehner, F.K., 1995. A model of intergranular pressure solution in open systems. Tectonophysics 245, 153–170.
Martin, B., Roller, K., Stockhert, B., 1999. Low-stress pressure solution experiments on halite single-crystals. Tectonophysics 308, 299–310.
Oelkers, E.H., Bjorkum, P.A., Murphy, W.M., 1996. A petrographic and computational investigation of quartz cementation and porosity reduction in North Sea sandstones. American Journal of Science 296, 420–452.
Onasch, C.M., 1993. Determination of pressure solution shortening in sandstones. Tectonophysics 227, 145–159.
Onasch, C.M., 1994. Assessing brittle volume-gain and pressure solution volume-loss processes in quartz arenite. Journal of Structural Geology 16, 519–530.
Onasch, C.M., Shen-Tu, B., Couzens-Schultz, B.A., 1998. Strain partitioning and factorization in quartz arenite. Journal of Structural Geology 20, 1065–1074.
Peacock, D.C.P., Sanderson, D.J., 1995. Pull-aparts, shear fractures and pressure solution. Tectonophysics 241, 1–13.
Railsback, B.L., 1993. Lithologic controls on morphology of pressure-dissolution surfaces (stylolites and dissolution seams) in Paleozoic carbonate rocks from the mideastern United States. Journal of Sedimentary Petrology 63, 513–522.
Renard, F., Ortoleva, P., Gratier, J.-P., 1997. Pressure solution in sandstones: influence of clays and dependence on temperature and stress. Tectonophysics 280, 257–266.
Renard, F., Dsythe, D.K., 2003. In: Middleton, G.V. (Ed.), Encyclopedia of Sediments and Sedimentary Rocks. Kluwer Academic Publishers, pp. 542–543.
Renard, F., Schmittbuhl, J., Gratier, J.-P., Meakin, P., Merino, E., 2004. Three-dimensional roughness of stylolites in limestone. Journal of Geophysical Research 109, B0329. doi:10.1029/2003JB002555.
Rossi, M., Vidal, O., Wunder, B., Renard, F., 2007. Influence of time, temperature, confining pressure and fluid content on the experimental compaction of spherical grains. Tectonophysics 441, 47–65.
Rudnicki, J.W., 2007. Models for compaction band propagation. In: David, C., Le Ravalec-Dupin, M. (Eds.), Rock Physics and Geomechanics in the Study of Reservoirs and Repositories. Geological Society of London Special Publication, 284, pp. 107–125.
Rutter, E.H., 1983. Pressure solution in nature, theory and experiment. Journal of the Geological Society of London 140, 725–740.
Rutter, E.H., Wanten, P.H., 2000. Experimental study of the compaction of phyllosilicate-bearing sand at elevated temperature and with controlled pore water pressure. Journal of Sedimentary Research 70, 107–116.
Sarfaricz, M., Davison, I., 2005. Pressure solution in chalk. American Association of Petroleum Geologists Bulletin 89, 383–401.
Schmittbuhl, J., Renard, F., Gratier, J.P., 2004. Roughness of stylolites: implications of 3D high resolution Topography measurements. Physical Review Letters 93, 238501.
Sleeman, A.G., Pracht, M., 1994. Geology of South Cork. Geological Survey of Ireland. 58pp.
Sorby, H.C., 1864. On direct correlation of mechanical and chemical forces. Proceedings of the Royal Society 12, 538–550.
Sprunt, E.S., Nur, A., 1976. Reduction of porosity by pressure solution; experimental verification. Geology 4, 463–466.
Sternlof, K.R., Rudnicki, J.W., Pollard, D.D., 2005. Anticrack inclusion model for compaction bands in sandstone. Journal of Geophysical Research 110, B11403,. doi:10.1029/2005JB003764.
Sternlof, K.R., 2006. Structural Geology, Propagation Mechanics and Hydraulic Effects of Compaction Bands in Sandstone. Ph.D. thesis. Stanford University.
Stockdale, B., 1922. Stylolites: Their Nature and Origin, IX. Indiana University Studies. 97pp.
Van Noort, R., Spiers, C.J., 2009. Kinetic effects of microscale plasticity at grain boundaries during pressure solution. Jounal of Geophysical Research 114, B03206. doi:10.1029/2008JB005634.
Weyl, P.K., 1959. Pressure solution and the force of crystallization – A phenomenological theory. Journal of Geophysical Research 64, 2001–2025.
Yang, X., 2000. Pressure solution in sedimentary basins: effect of temperature gradient. Earth and Planetary Science Letters 176, 233–243.
Zhou, X., Aydin, A., 2010. Mechanics of pressure solution growth and evolution. Journal of Geophysical Research 115, B12207. doi:10.1029/2010JB007614.